

Influence of Pr on Natural Convection Heat Transfer of an Open Channel Finned Plate

Seung-Hyun Hong and Bum-Jin Chung*

Department of Nuclear Engineering, Kyung Hee University
#1732 Deokyoungdae-ro, Giheung-gu, Yongin-si, Gyeonggi-do, 446-701, Korea
*Corresponding author: bjchung@khu.ac.kr

1. Introduction

The passive cooling system by natural convection gains research interests for the nuclear systems, after the Fukushima NPP accident. The finned plate provides the extended heat transfer area and improves the heat transfer. However when the fin spacing becomes small, the pressure drop increases due to frictional loss, heat transfer is impaired. Thus there is an optimal fin spacing.

For the natural convection heat transfer, the heated thermal boundary layer drives the flow and the influence of the Prandtl number on the heat transfer will be very important as the thickness of the thermal boundary layer depends on it.

This study aims at investigating the influence of the Prandtl number on the natural convection heat transfer of the finned plate. Numerical analyses were performed by varying the Pr from 2 to 2,014.

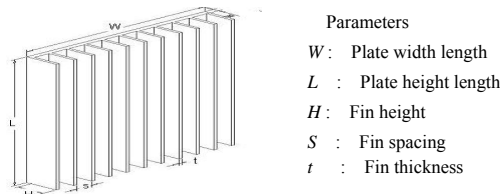


Fig. 1. Parameters of rectangular plate fin.

2. Previous studies

Natural convection heat transfer phenomena for vertical plates are well known and many heat transfer correlations have been developed. For the laminar natural convection, Bejan [1] performed the scale analysis from governing equations and proposed a scale relation. Le Fevre suggested the Equation (1) for the laminar natural convection heat transfer correlation for vertical plates [2].

$$Nu_H = 0.67(Gr_H Pr)^{1/4} \quad \text{at} \quad Gr_H < 10^9 \quad (1)$$

Starner and McManus [3] presented heat transfer coefficients of four differently dimensioned fin arrays with the vertical base plate. They showed that incorrect application of fins to a surface actually may reduce the total heat transfer to a value even below that of the base alone.

Welling and Wooldridge [4] have studied heat transfer from plate-fin heat sinks experimentally. They

reported optimum values of the ratio of fin height to spacing.

3. Numerical Simulations

3.1 Test matrix

The original configuration of the finned plate is summarized as follows; Fin height (H) 0.005m, Fin spacing (S) 0.002m, and Plate Length (L) 0.05m. Fig. 2

shows the simulated geometry.

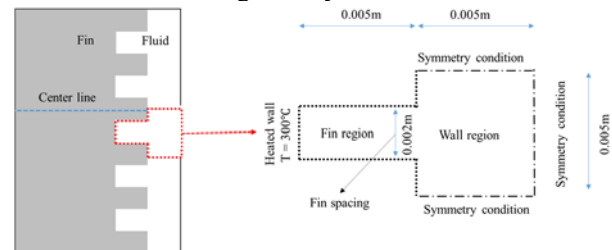


Fig. 2. Plane view of the simulated geometry.

As the study is performed as the complementary study for other experimental work, the material properties used in the study are the same as the work. Only the values of Prandtl number were varied: 2, 20, 200, and 2,014.

Table 1. Material properties.

Density (kg/m ³)	1096.5555
Cp (J/kg-k)	1000
K (W/m K)	6.225 × 10 ⁻⁰⁴
Viscosity (kg/ms)	1.253 × 10 ⁻⁰³
B (1/K)	5.613 × 10 ⁻⁰⁵
Pr	2~2014
Ra _L	1.05 × 10 ⁷ ~1.05 × 10 ¹⁰

3.2 Simulation Methods

Governing equations and boundary conditions are listed in Equations (1)-(6).

$$\frac{\partial u_i}{\partial x} + \frac{\partial u_j}{\partial y} + \frac{\partial u_k}{\partial z} = 0. \quad (1)$$

$$u_i \frac{\partial u_i}{\partial x} + u_j \frac{\partial u_i}{\partial y} + u_k \frac{\partial u_i}{\partial z} = \nu \left(\frac{\partial^2 u_i}{\partial x^2} + \frac{\partial^2 u_i}{\partial y^2} + \frac{\partial^2 u_i}{\partial z^2} \right) - \frac{1}{\rho} \frac{\partial p}{\partial x}, \quad (2a)$$

$$u_i \frac{\partial u_j}{\partial x} + u_j \frac{\partial u_j}{\partial y} + u_k \frac{\partial u_j}{\partial z} = \nu \left(\frac{\partial^2 u_j}{\partial x^2} + \frac{\partial^2 u_j}{\partial y^2} + \frac{\partial^2 u_j}{\partial z^2} \right) + g\beta, \quad (2b)$$

$$u_i \frac{\partial u_k}{\partial x} + u_j \frac{\partial u_k}{\partial y} + u_k \frac{\partial u_k}{\partial z} = \nu \left(\frac{\partial^2 u_k}{\partial x^2} + \frac{\partial^2 u_k}{\partial y^2} + \frac{\partial^2 u_k}{\partial z^2} \right) - \frac{1}{\rho} \frac{\partial p}{\partial z}. \quad (2c)$$

$$u_i \frac{\partial T}{\partial x} + u_j \frac{\partial T}{\partial y} + u_k \frac{\partial T}{\partial z} = \alpha \left(\frac{\partial^2 T}{\partial x^2} + \frac{\partial^2 T}{\partial y^2} + \frac{\partial^2 T}{\partial z^2} \right). \quad (3)$$

$$u_i = u_j = u_k = 0 \quad \text{at all the walls.} \quad (4)$$

$$T = T_0 \quad \text{on heated wall.} \quad (5)$$

$$T = T_\infty \quad \text{as fluid.} \quad (6)$$

The numerical analysis was performed using FLUENT ver. 6.3.26 [5].

The simulations were carried out using the Boussinesq approximation. The temperature of the heated walls was maintained at 400 K to provide a constant temperature condition. The segregated solver was used with a second-order upwind algorithm for momentum and energy in the laminar model. For pressure discretization, the standard algorithm was adopted, whereas the SIMPLE algorithm was used for pressure-velocity coupling discretization.

The optimized cell number of about 2.4×10^5 cells, was obtained by performing a sensitivity analysis.

4. Results and Discussion

4.1 Comparison with Le Fevre correlation

The results were compared with Le Fevre natural convection heat transfer correlation for vertical plates. In order to compare the results with flat plates, the total heat transfer rates were divide by the whole surface area so that the Nu_L 's of the finned plates were compared with the Nu_L 's of the flat plates of the same areas.

Fig. 3 shows the result. As the Prandtl number increases, the difference between the flat plate and finned plate decrease. The increase of the Prandtl number, reduces the thickness of the thermal boundary layer and the interference between the thermal boundary layers formed at the base plate and the fin will be reduced.

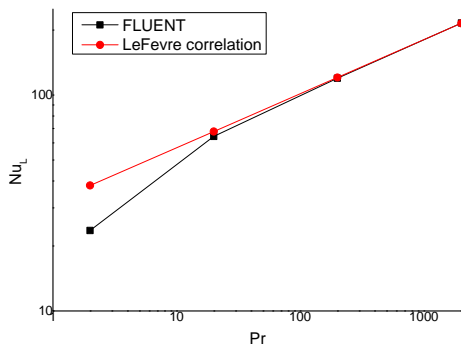


Fig. 3. Comparison with the Flat Plates of the Same Areas.

4.2 Velocity profiles

Fig. 4 presents the velocity profiles at each elevation for four different Pr values. The developments of the momentum boundary layers along the elevation can be observed. The smaller the Pr, the boundary layer starts to develop early.

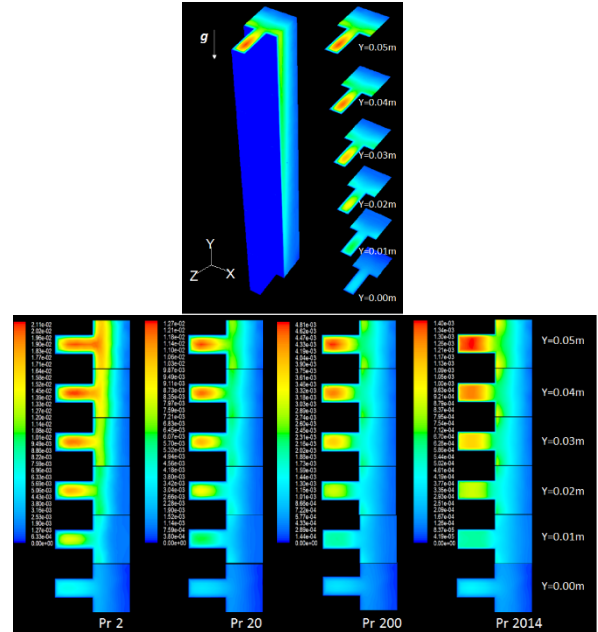


Fig. 4. Velocity profiles for each elevation.

Fig. 5 shows the cross-sectional velocity profiles along the flow direction chopped at the center line between the fins. This also shows almost similar velocity profiles. The early start of the boundary layer development for small Pr can be more easily seen.

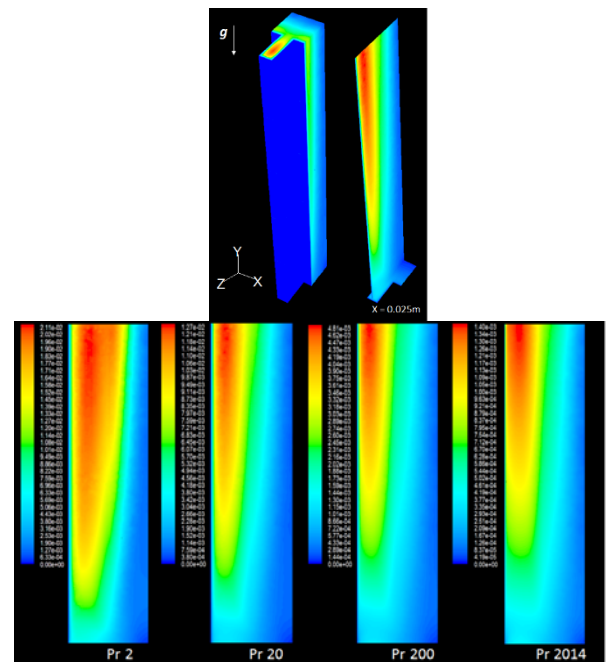


Fig. 5. Velocity profiles along the flow direction.

4.3 Temperature profiles

Fig. 6 presents the temperature profiles at each elevation for four different Pr values. The developments of the thermal boundary layers along the elevation depend strongly on the Pr values.

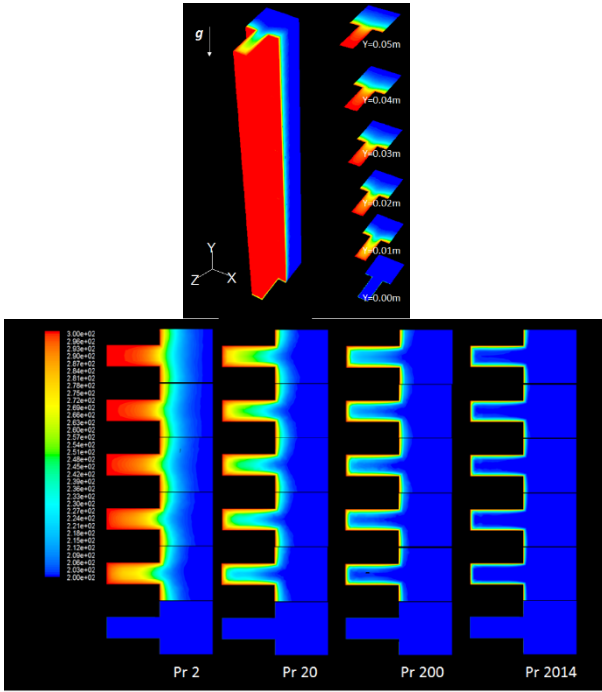


Fig. 6. Temperature profiles for each elevation.

The larger the Prandtl number, the thinner the thermal boundary layer. The similar observation can be made by Fig. 7, which shows the cross-sectional temperature profiles along the flow direction chopped at the center line between the fins.

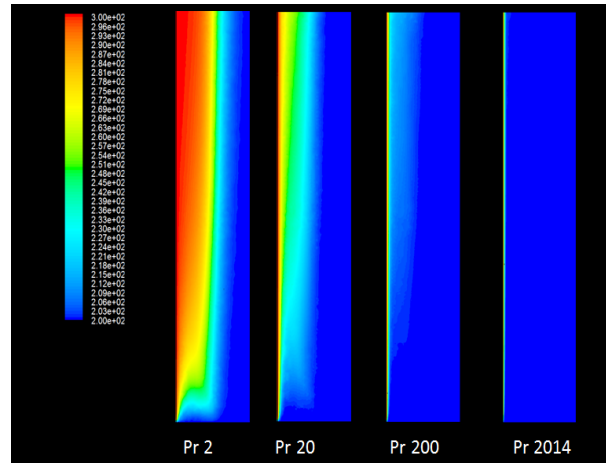
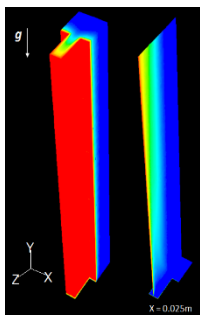


Fig. 7. Temperature profiles along the flow direction.

An extremely thin thermal boundary layer is observed for the Prandtl number of 2,014. This means that the interference between the thermal boundary layers developed from the base plate and the fin will be reduced and thus the heat transfer behavior will become similar to that of the flat plate of the same area as shown in Fig. 3.

5. Conclusions

Numerical analysis was performed for the natural convection heat transfer of a finned plate in an open channel. In order to investigate the influence of the Prandtl number on the heat transfer, four different values of Prandtl numbers were simulated and compared.

As expected, the velocity profiles were almost similar except for the fact that the boundary layer develops earlier for smaller Prandtl number fluid. However the temperature profiles varied drastically depending on the values of the Prandtl number. As the Prandtl number increases, the thermal boundary layer reduces.

The comparisons of the results with Le Fevre natural convection heat transfer correlation for vertical plate shows that as the Pr increases, the Nu_L of the finned plate becomes similar to that of the flat plate of the same heat transfer area.

6. REFERENCES

- [1] A. Bejan, Convection Heat Transfer, 2nd ed., John Wiley & Sons, INC, New York, pp. 466-514, 1994.
- [2] E.J. Le Fevre, Laminar Free Convection From a Vertical Plane Surface, 9th International Congress on Applied Mechanics, Brussels, Vol. 4, pp. 168-174, 1956.
- [3] K.E. Starner, H.N. McManus Jr., An experimental investigation of free-convection heat transfer from rectangular-fin arrays, Journal of Heat Transfer, Vol. 85, pp. 273-278, 1963.

- [4] J.R. Welling, C.B. Wooldridge, Free convection heat transfer coefficients from rectangular vertical fins, *Journal of Heat Transfer*, Vol. 87, pp. 439-444, 1965.
- [5] *Fluent User's Guide* (2006) release 6.3 Fluent Incorporated.